Catalysis Today 155 (2010) 199–205

Contents lists available at ScienceDirect

Catalysis Today

journal homepage: www.elsevier.com/locate/cattod

Structure of alumina supported platinum catalysts of different particle size during CO oxidation using in situ IR and HERFD XAS

Jagdeep Singh, Jeroen A. van Bokhoven *

Institute for Chemical and Bioengineering, ETH Zurich, 8093 Zurich, Switzerland

ARTICLE INFO

Article history:
Available online 15 January 2010

Keywords:
HERFD XAS
IR spectroscopy
CO oxidation
Pt/Al_2O_3
Particle size effect

ABSTRACT

The structure of alumina supported platinum catalysts has been studied using in situ time-resolved high-energy resolution fluorescence X-ray absorption spectroscopy (HERFD XAS), in situ infrared (IR) spectroscopy, and kinetic measurements during CO oxidation at O_2 to CO ratio of one. Regardless of the particle size, the CO oxidation occurred in two distinctive regimes, a high-activity regime and a low-activity regime, which have high and low rates of reaction respectively, as observed in previous studies. The size of the particles slightly affects the rate in the low-activity regime, which was more difficult to assess in the high-activity regime. The catalyst surface is poisoned by adsorbed CO in the low-activity regime, as probed by HERFD and IR, and in the high-activity regime, the catalyst exhibits higher activity paralleled with the formation of a surface oxide.

1. Introduction

The CO oxidation over platinum is one of the most studied catalytic reactions in the field of heterogeneous catalysis. One of the main aims in these studies of heterogeneous catalysis is to understand and relate the observed catalytic behaviour of the metal particles to the structure and geometry of the particles on their respective supports. This allows optimizing the synthesis of better catalysts. The electronic properties of the metal, which varies drastically with cluster size and shape [1–6], play a vital role in many industrial processes such as preferential oxidation (PROX) of CO in a hydrogen-rich mixture for the technical purification of the hydrogen feed gas [7] and in automotive applications [8]. The observed particle size effect [9–18] during CO oxidation has been well documented and related to the reaction rate and experimental conditions. The structure sensitivity of the CO oxidation has been well established for platinum single crystals under high vacuum conditions, and for catalysts with varying platinum nanoparticle sizes [19–23], which amongst others has been related to the higher reaction rate on terrace sites in comparison to the defect sites (steps and kinks). Adsorbed CO on plane surfaces is shown to be more reactive than adsorbed on low coordination sites [12]. Reaction turnover frequencies increase with increasing particle size [24,28].

The knowledge of the atomic-level structure of catalytic active sites is important to determine the activity of these noble metal catalysts. The active species on supported catalysts are still uncertain. There have been many studies claiming that metallic platinum is the active surface species for CO oxidation even in an O_2-rich environment [25–28]. Recent surface diffraction studies on surfaces of platinum single crystals [29] on the other hand, indicate that the rate of CO oxidation is higher when the surface is oxidized. It has also been suggested that the active structure is a combination of metallic and oxidic phases on the supported metal catalysts [30,31]. Theoretical calculations have shown the role played by partially oxidized surfaces in generating high catalytic activity [32–35]. Scanning tunneling microscopy revealed the high reactivity of an O_2-rich ruthenium surface in the oxidation of carbon monoxide [36].

The CO oxidation on single crystals [26,29,37] and supported platinum catalysts [38–42] occurs in two reaction regimes respectively with low and high reaction rates at O_2 to CO ratios greater than stoichiometric. The low-activity state is characterized by the adsorbed CO that poisons the active surface [25,38,43,44]. The high-activity state is characterized by the presence of a surface oxide [29,41,42]. Most of the studies had applied IR spectroscopy to probe the active sites during the reaction. Despite these extensive studies [25,43,45–47], there is little agreement concerning the role of carbonyl species in the CO oxidation. There are reports where linear and bridged adsorbed CO are shown to be active [25] and reports where bridged adsorbed carbonyl species are more active for CO oxidation [48]. The co-adsorbed CO with oxygen atom is also shown to be responsible for the formation of carbon dioxide [45]. Also, the existence of islands on the catalyst

* Corresponding author at: Institute for Chemical and Bioengineering, Department of Chemistry and Applied Biosciences, HCI E 127, Wolfgang Paulistrasse 10, 8093 Zurich, Switzerland. Tel.: +41 446325542; fax: +41 446321162.
E-mail address: j.a.vanbokhoven@chem.ethz.ch (J.A. van Bokhoven).

0920-5861/$ – see front matter © 2009 Elsevier B.V. All rights reserved.
doi:10.1016/j.cattod.2009.12.006

surface has been shown [44,49] to be relevant for CO oxidation, the formation of which is dependent on the particle morphology and size [50].

In this work, we have studied the structure of working supported platinum catalysts of different particle sizes in a plug-flow reactor, combining time-resolved X-ray absorption spectroscopy (XAS), infrared (IR) spectroscopy, and kinetic measurements by means of mass spectrometry. In situ IR spectroscopy provides the information of the adsorbed species on the metal surfaces during the reaction conditions. As the adsorption of reactants and intermediates on the surface of transition metals involves the interaction of the atomic or molecular orbitals of the adsorbate with the bands on the metal, it is important and relevant to study the state of the metal itself during the reaction and detect the orbitals that are involved in bonding reactants. In situ XAS provides the local electronic and geometric structure of the platinum species during CO oxidation. The intensity of the whiteline of an L_3-edge XAS spectrum reveals the unfilled d band and is sensitive to the metal oxidation state and presence of adsorbates on the surface. The shape of the spectrum reveals the mode of adsorption [51–54]. The use of high-energy resolution fluorescence X-ray absorption spectroscopy (HERFD XAS) improves the resolution of the spectra [54–57]. The sharper features in these spectra originate from the broadening of a smaller final state core-hole lifetime of a particular fluorescence channel, as detected by a secondary energy-selective spectrometer [55,57]. Therefore, HERFD XAS provides more insight into the geometric and electronic structures of the active metal and IR spectroscopy provides the insight into the surface species present on the active sites. We have established the influence of particle size on the rate of CO oxidation and on the structure of platinum under the reaction conditions.

2. Experimental

2.1. Catalyst synthesis

1.90 wt% Pt/Al_2O_3 was synthesized using the incipient-wetness impregnation method. 1.0 g $Pt(NH_3)_4(NO_3)_2$ was added to 25 g of γ-alumina, which had surface area of 180 m^2/g, in 14 mL deionized water. 2 mL concentrated NH_4OH was later added to the above mixture. The sample was then dried overnight at 398 K, for 3 h at 498 K, and reduced at 523 K in a flow (100 mL/min) of pure hydrogen at atmospheric pressure. The Pt elemental composition was determined by the inductively coupled plasma method. One batch of the catalyst was calcined at 623 K and another batch at 773 K, both in the presence of static air. The catalysts calcined at 623 and 773 K will be mentioned, further in this work, as Pt-623 and Pt-773 respectively.

2.2. Electron microscopy

The particle size and size distribution were determined by scanning transmission electron microscopy (STEM). The sample was retained on a carbon foil after the evaporation of ethanol. The measurements were performed, using a copper grid supporting the sample, using a Tecnai F30 microscope operating with a field-emission cathode operated at 300 kV using a high-angle annular dark-field (HAADF) detector. Platinum particles were detected as the bright spots in the STEM micrographs as confirmed by energy-dispersive X-ray spectroscopy (EDX).

2.3. Kinetic measurements

The experiments were conducted using the flow scheme as described elsewhere [58]. The gas flow rates were controlled using computer controlled mass flow controllers (MFCs). The reactor [59], which resembled a plug-flow reactor with a diameter of 1.6 mm, was equipped with a transmission/fluorescence cell with aluminum windows to allow XAS experimentation. The temperature of the catalyst system was monitored by a thermocouple in the reactor holder. The catalyst, with a sieve fraction of 63–125 μm particles, weighing approximately 19 mg, was pre-treated in situ in 5% hydrogen in helium at 473 K before each experiment and cooled down in a flow of pure helium. After pre-treatment, the oxidation reaction was carried out in an atmosphere of CO and O_2 with O_2 to CO ratio of one. The outlet from the reactor was connected to a GSD Omnistar mass spectrometer from Pfeiffer Vacuum to monitor the gases. The measurements were done at a constant total flux of 30 N mL/min through the reactor corresponding to a space velocity of about 64,000 h^{-1}. For calculating rate of CO_2 production, the traces for CO, O_2, and CO_2, recorded by the mass spectrometer in terms of current, were divided by He signal for normalization. Assuming a linear correlation between CO conversion and normalized signal of CO_2, with boundary conditions of no CO conversion at the start of reaction and 100% CO conversion after ignition temperature, CO conversion was calculated from the mass spectrometer signals. The rate of CO_2 production was calculated from the CO conversion afterwards.

2.4. High-energy resolution fluorescence detected (HERFD) X-ray absorption spectroscopy

X-ray absorption experiments were carried out at an undulator beamline ID26 at the European Synchrotron Radiation Facility (ESRF), Grenoble, France, which is operated at the energy of 6.0 GeV, and the ring current varying between 50 and 90 mA. The X-ray beam measured 0.3 mm horizontal and 1 mm vertical; the total flux was 5×10^{12} photons/s. The energy was calibrated with a Pt foil. The incident energy was monochromatized using a pair of Si(1 1 1) crystals with an energy bandwidth of 1.5 eV at the Pt L_3-edge. Higher harmonics were suppressed by using two mirrors, one coated with Pd and the other with Cr, working at 3 mrad in total reflection. High-energy resolution emission detection was carried out with a horizontal-plane Rowland circle spectrometer that was tuned to the Pt $L\alpha_1$ (9442 eV) fluorescence line. A total energy bandwidth (incident energy convoluted with emission detection) of 1.8 eV was achieved with the (6 6 0) Bragg reflection of one spherically bent Ge wafer (R = 1000 mm). The detector was an avalanche photodiode (APD). A Canberra silicon photodiode was mounted to measure the total fluorescence simultaneously with the HERFD XAS. Spectra were collected before and during heating of the sample at 2 K/min to the temperature of maximum conversion; the ratio of O_2 to CO was one corresponding to an O_2-rich environment. The spectra were collected with a time resolution of 90 s.

2.5. IR spectroscopy

In situ IR measurements were made using a Bio-Rad spectrometer. The detector was a cryogenic mercury cadmium telluride (MCT) with a maximum beam divergence of 1.3 mrad. The measurements were done on a self-supporting catalyst pellet of 15 mg. The IR beam transmitted through the sample. The catalyst was pre-treated prior to each experiment as explained in Section 2.3. The background spectrum was collected with catalyst at 313 K in a flow of 5% O_2 in He. The catalyst was then exposed to the reaction mixture with O_2 to CO ratio of one. The measurements were done, similar to XAS measurements, at a constant total flux of 30 mL/min through the reactor corresponding to a space velocity of about 64,000 h^{-1}. The pellet was heated at a rate of 2 K/min. The spectra were collected in continuous mode with time resolution of 5 s.

3. Results and discussion

The synthesis of catalysts resulted in well dispersed nanoparticles on alumina. Fig. 1 shows STEM micrographs of Pt-623, and Pt-773 catalysts. For Pt-773 the particle size ranged from 1 to 4 nm with maximum particles of about 2.3 nm in size. Pt-623 has a narrow size distribution of the platinum nanoparticles around 0.7 nm. The small bright spots were confirmed, by EDX, to be platinum particles supported on alumina, which was reflected as less bright texture in the STEM micrographs. These supported platinum nanoparticles after being exposed to the reaction mixture of CO and O_2 showed the conversion curves in CO when the catalyst bed was heated at 2 K/min. The runs were done in an O_2-rich environment, with O_2 to CO ratio of one. Fig. 2 shows the rate of CO_2 production for Pt-623 (black) and Pt-773 (red) that had been calculated from mass spectrometer traces of CO_2. From the figure, it is clear that both catalysts show two different reaction regimes namely high-activity regime and a low-activity regime. These regimes had been observed before also for single crystals [26,29,37] and supported platinum catalysts [38–42] under UHV and atmospheric pressure. The two regimes are separated by a sudden increase in the activity of the catalyst that results in the increase in rate of CO_2 production. This sudden jump in the activity is referred as "ignition". After the ignition, the catalyst does not show any increase in the rate of CO_2 production owing to 100% conversion of CO. Just after the ignition, before the catalyst goes in the regime of constant rate of reaction with high activity, there is an extra positive spike in CO_2 production, which is explained later. Noticeable is that intensity of this spike is higher in case of Pt-623 compared to Pt-773. After the onset of CO_2 production, around 380 K, Pt-623 always showed higher rate of reaction in comparison to Pt-773 for any particular temperature. The TOF was calculated using the dispersion, which was calculated from the particle size using an established correlation in the literature [69]. TOF for Pt-623 at 440 K was 0.02 s^{-1}, which was approximately 1.5 times that of Pt-773. Therefore, under O_2-rich conditions, in the low-activity region, the CO oxidation is sensitive to the structure of the catalyst [10,11,15,16]. The ignition temperature also strongly depended on the size of the platinum particles. Pt-623 showed ignition temperature of 476 K compared to 507 K in case of Pt-773. This implies that under similar reaction conditions, 0.7 nm platinum particles require lower temperature to ignite and go to the high-activity regime compared to 2.3 nm platinum particles supported on alumina. The catalysts showed different adsorption of CO in these two reaction regimes. Fig. 3(a) shows IR spectra that had been collected during the CO oxidation in O_2 to CO ratio of one. For clarity reasons, not all the spectra are shown which were collected at a time resolution of 5 s. At the start of the reaction, at about 330 K, the spectrum showed a pronounced peak at 2079 cm^{-1}, corresponding to stretching frequency of linearly absorbed CO on platinum [28,44,60] and a broad shoulder at 1838 cm^{-1}, which is assigned to stretching frequency of bridge-bonded CO on platinum particles [44,60]. The double peak between 2100 and 2200 cm^{-1} is due to the gaseous CO. The peak at 2250 cm^{-1} may be assigned to carbon monoxide multiply bonded to oxidized platinum sites [37]. As the

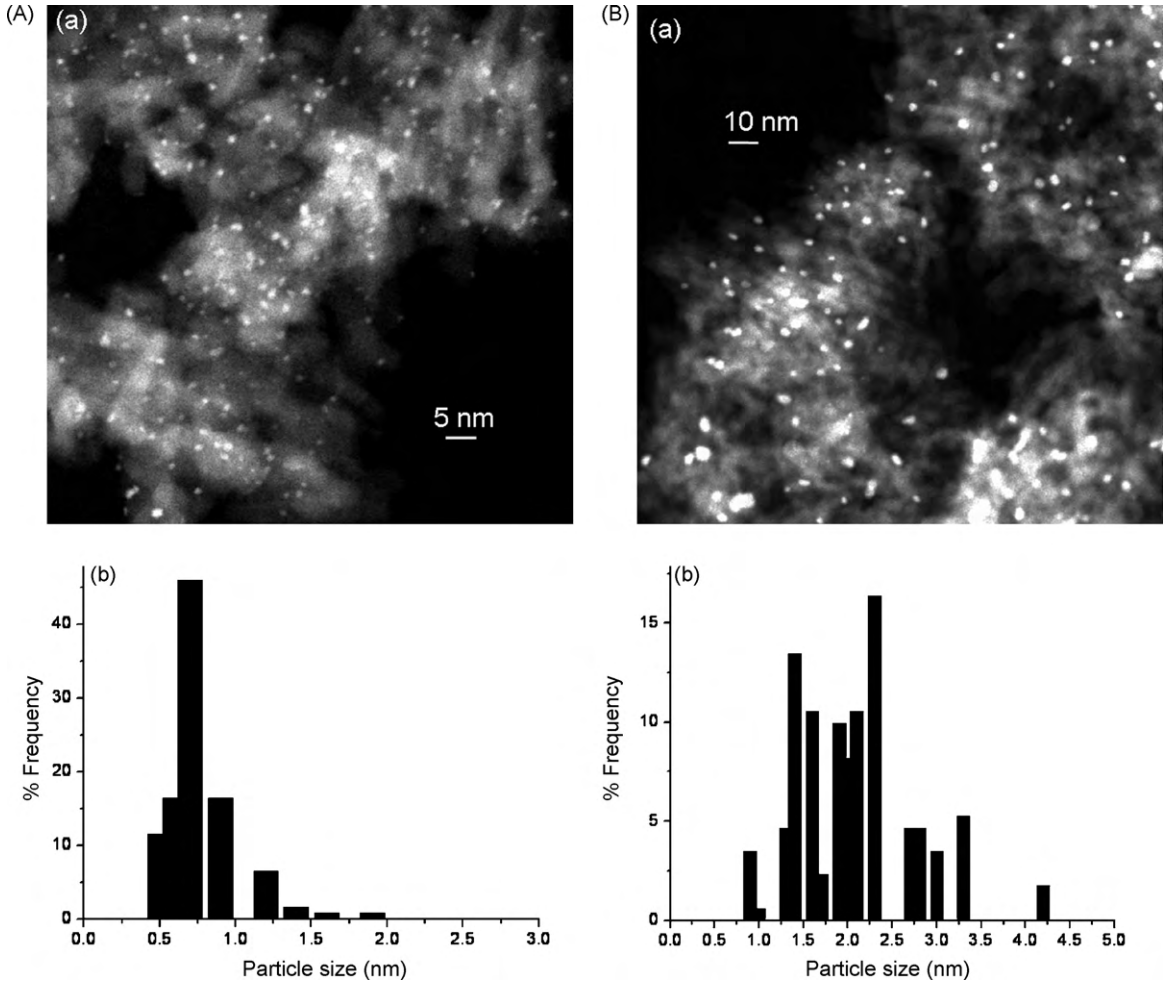

Fig. 1. (a) STEM micrograph of 2 wt% Pt/Al_2O_3 prepared by incipient-wetness impregnation and (b) particle size distribution of platinum particles for (A) Pt-623 and (B) Pt-773.

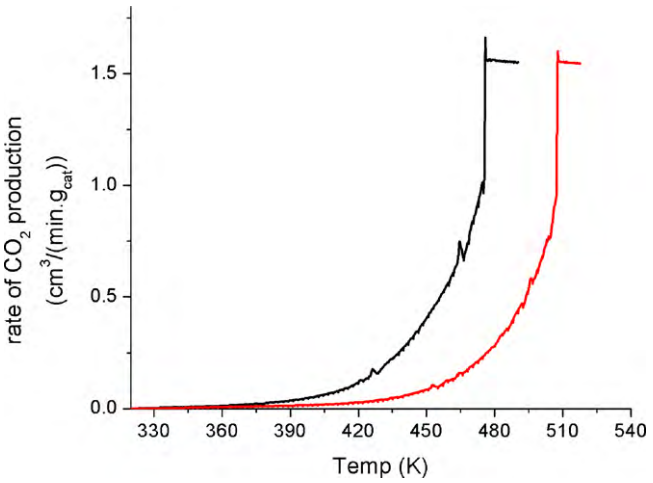

Fig. 2. Rate of CO oxidation during heating at O_2 to CO ratio of one over Pt-623 (black) and Pt-773 (red). (For interpretation of the references to color in this figure legend, the reader is referred to the web version of the article.)

temperature was increased, the spectrum changed. The peak at 2079 cm^{-1}, assigned to linearly adsorbed CO was shifted to lower wavenumber. However, the intensity of the peak decreased slightly until 486 K. The peak shift is well known and had been observed before on supported platinum catalysts and single crystals [44,49,61–63]. This shift emerges from two contributions; dipole–dipole interaction and temperature. The dipole–dipole interaction of adjacent CO molecules on the platinum surface affects the frequency of vibration. The vibrational frequency increases with increase in the density of CO dipoles on the surface. The similar explanation holds for the blue shift of bridged CO frequency on platinum with increase in temperature. The peak at 2350 cm^{-1}, assigned to gaseous CO_2 species appeared at 406 K. The intensity of this peak increased with increase in temperature up to 486 K. The spectrum at 493 K showed a sudden increase in intensity at 2350 cm^{-1} and a large drop in the intensities of 2079 and 1838 cm^{-1}, suggesting a sudden drop in the adsorbed CO species on platinum surface parallel to increase in CO_2 production. This sudden "ignition" as explained above, occurred at 490 K. Fig. 3(b) shows the changes in the mass spectrometer traces collected at the end of the reactor with increase in temperature. Also, the peak areas of linearly adsorbed and bridged CO, calculated from the spectra shown in Fig. 3(a), are plotted. Mass spectrometer signals of CO and O_2 started to decrease with increase in temperature resulting in CO_2 production as shown by increase in CO_2 signal. The peak area of linearly adsorbed CO shows a slight increase with increase in temperature. This increase may originate either from the discrepancy in calculation of peak areas at different temperatures as only one background was collected at 313 K or from the fluctuations in the baseline at higher temperatures as observed for supported platinum catalysts, resulting in broadening of the peak around 2000 cm^{-1} [44] or from the changes in the extinction coefficient with temperature. The peak area of bridged CO decreases with increase in temperature suggesting the desorption of CO from the surface. The changes in the peak areas of adsorbed CO paralleled mass spectrometer signals with increase in temperature. Just after ignition, CO and O_2 signals dropped and CO_2 signal increased suddenly and became constant in the high-activity region. This sudden change was in parallel with the drop in the peak areas of linearly adsorbed and bridged CO on the platinum surface. This clearly suggests that in the low-activity region adsorbed CO poisons the active surface and does not allow the catalyst to exhibit high activity [38,41,42,44]. This active surface was observed and characterized using X-ray absorption spectroscopy, whose results are shown in the later part of this section. The desorption of this adsorbed CO is the rate-determining step in this low-activity region [26,43,44,47]. Once the catalyst surface is free of CO, after ignition, the catalyst has the ability to display a higher activity [29,41,64].

Similar results were obtained for the Pt-623 catalyst. Fig. 4(a) shows the IR spectra at various temperatures acquired during heating the catalyst in an environment of O_2 to CO ratio of one. Comparing the spectrum in the low-activity region, at about 350 K, with Pt-773 sample, the peak of linearly adsorbed CO is blue shifted to 2063 cm^{-1}. Such differences have been observed [65], depending on the dispersion of platinum particles. With decrease in particle size, average number of platinum–platinum bonds per platinum atom decreases [66], resulting in different hybridization between s, p, and d orbitals. This may result in weakening of the C–O bond due to more back bonding into the $2\pi^*$ orbital of adsorbed CO that further results in lower stretching frequency of adsorbed CO. Also, a change in dipole–dipole interaction because of different island sizes may contribute to this shift. The results also agreed with the explanation of lower CO stretching frequency with lower coordination sites (corners and edges) of platinum atoms [67,68]. The blue

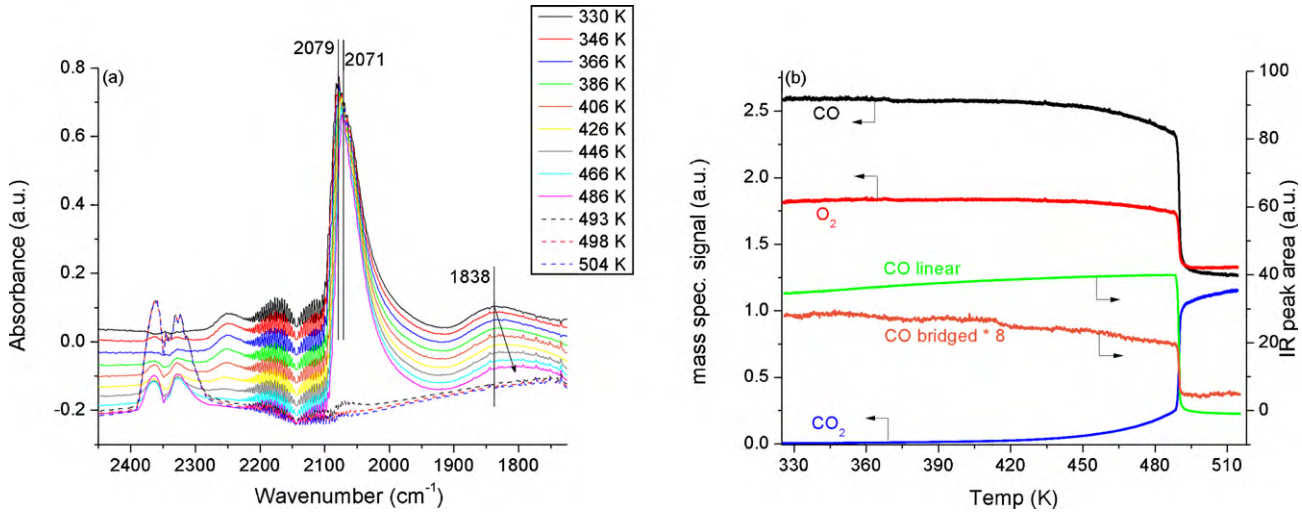

Fig. 3. (a) IR spectra of Pt-773 in a pellet reactor at O_2 to CO ratio of one at 330 K (solid black), 346 K (solid red), 366 K (solid blue), 386 K (solid green), 406 K (solid orange), 426 K (solid yellow), 446 K (solid grey), 466 K (solid cyan), 486 K (solid pink), 493 K (dash black), 498 K (dash red), and 504 K (dash blue); ignition occurred at 490 K; (b) mass spectrometer traces of CO, O_2, and CO_2, and peak areas of linearly adsorbed and bridged CO. (For interpretation of the references to color in this figure legend, the reader is referred to the web version of the article.)

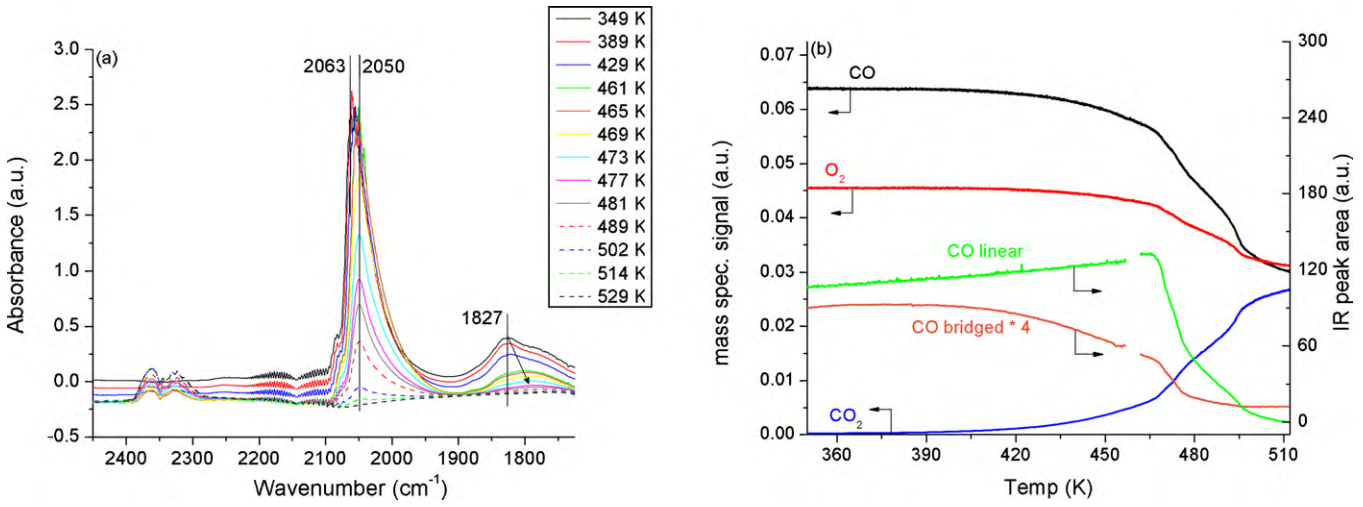

Fig. 4. IR spectra of Pt-623 in pellet reactor at O_2 to CO ratio of one at 349 K (solid black), 389 K (solid red), 429 K (solid blue), 461 K (solid green), 465 K (solid orange), 469 K (solid yellow), 473 K (solid cyan), 477 K (solid pink), 481 K (solid grey), 489 K (dash red), 502 K (dash blue), 514 K (dash green), and 529 K (dash black); (b) mass spectrometer traces of CO, O_2, and CO_2, and peak areas of linearly adsorbed and bridged CO. (For interpretation of the references to color in this figure legend, the reader is referred to the web version of the article.)

shift of bridged CO results in the peak at 1827 cm^{-1} in comparison to 1838 cm^{-1} in case of Pt-773 sample. The higher fraction of these lower coordination sites (surface atoms) of platinum atoms in case of Pt-623 may explain the higher spike in CO_2 production (Fig. 2) just after ignition for 0.7 nm particles (Pt-623) in comparison to 2.3 nm particles (Pt-773). Because 0.7 nm particles have a higher surface area, more CO is adsorbed on the catalyst with small particle compared to the one with 2.3 nm particles, and is reacted away to form the additional CO_2. Also, because ignition occurred at lower temperature in case of Pt-623 compared to Pt-773, less CO is desorbed from the surface. Although, no clear ignition was observed, as shown in Fig. 4(b), for Pt-623 sample in the IR cell with catalyst as a self-supporting pellet, the trend of loss of adsorbed CO from the surface is very similar to that of Pt-773 sample. In the low-activity region, up to approximately 470 K, platinum surface was covered by CO. With increase in temperature, the peaks at 2063 and 1827 cm^{-1} were blue shifted (Fig. 4(a)) as explained above. After about 470 K, the mass spectrometer signals of CO and O_2 showed a decrease which is sharper than the decrease below 470 K. Parallel to this there was an increase in CO_2 signal. The peak areas of CO adsorbed both linearly and bridged followed exactly the trend of the mass spectrometer signals. As there was no sudden ignition observed in this case, the surface was never free totally from CO. This can be observed from the observed peak of linearly adsorbed CO in Fig. 4(a). As the intensity of the peak of adsorbed CO goes down, during ignition there is no shift in the peak position which might suggest a constant island size and that particles are freed from CO one by one. Ultimately in the high-activity region, some CO remained adsorbed to poison the catalyst, however, a high-activity part of the catalyst coexisted. The evolution of CO_2 peaks also confirms the formation of more active surface at these prevailing conditions.

To probe the structure sensitivity and to determine the structure of the catalyst in the low- and high-activity regimes, in situ HERFD XAS was applied. The HERFD XAS technique provides complementary information to that obtained from the vibrational techniques; i.e. gives the geometric and electronic structures of the catalytic metal site during reaction. Therefore, with this technique the electronic structure of platinum was determined and is explained under different reaction conditions for the two samples with different particle sizes. Fig. 5(a) shows the Pt L_3-edge HERFD XAS spectra of Pt-623 measured between 300 and 490 K in an atmosphere of O_2 and CO at a ratio of one. The spectra were recorded while measuring the conversion plot of Fig. 2. Below 470 K, the spectra shows a pronounced doublet in the whiteline,

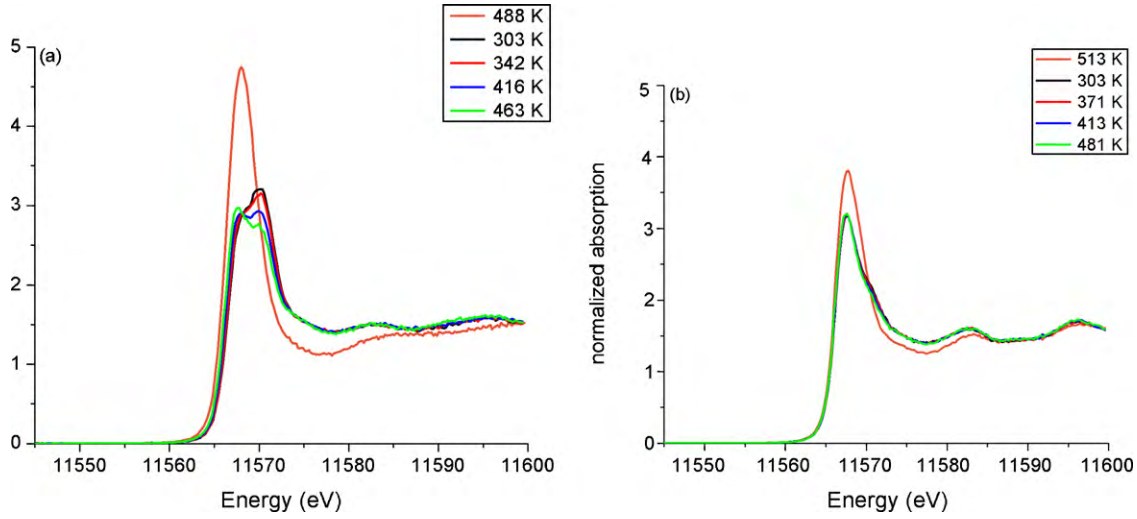

Fig. 5. Pt L_3-edge HERFD XANES of (a) Pt-623 and (b) Pt-773 during CO oxidation at O_2 to CO ratio of one measured during heating in plug-flow reactor.

which is characteristic of adsorbed CO [54]. The doublet feature in the HERFD spectrum corresponds to the atop adsorbed CO on platinum and it emerges due to the formation of anti-bonding state above the Fermi level through overlap of platinum d-orbitals and $2\pi^*$ of the C and O atoms [54]. This observation of adsorbed CO on reduced platinum is in agreement with our and others' IR data [25,28,43,44]. At temperatures below the ignition point, traces of CO are sufficient to completely reduce a pre-oxidized platinum catalyst even in the presence of an excess of O_2 [28,44,67]. CO thus poisons the catalyst surface and prevents it from oxidation even under an overdose of O_2 at sufficiently low temperature. As the temperature increased, the intensity of the doublet decreased and the edge shifted to lower energy, indicating desorption of CO at elevated temperatures [41]. At 487 K, a higher temperature than the ignition temperature, the spectra showed a strong increase in the intensity of the whiteline while the edge energy shifted, which is characteristic of partially oxidized platinum [54]. In our previous study [42], above the ignition temperature, the EXAFS analysis had shown that there is a loss of Pt–Pt contribution and appearance of Pt–O and a Pt–Pt contribution had a bond length that is characteristic of an oxide. Also, we observed that a platinum core remained. At this point, the conversion of CO was complete (Fig. 2). The XAS spectra showed no further changes at higher temperatures. Fig. 5(b) shows the Pt L_3-edge HERFD XAS spectra of Pt-773 measured between 300 and 515 K in an atmosphere of O_2 and CO at a ratio of one. The spectra in the low-activity region, below 500 K, are very different from Pt-623. The doublet feature in the whiteline, characteristic of atop adsorbed CO is not observed. However there is a small shoulder in the whiteline at around 11,570 eV. This shoulder is assigned as the same signature of atop CO on the platinum surface. The intensity of the surface adsorbed CO signature is low due to the much lower fraction of the surface atoms, as explained above. The intensity of this shoulder decreased with increase in temperature suggesting the desorption of CO. At temperature above ignition temperature of 507 K, the intense whiteline suggested the presence of a fraction of oxidized platinum which paralleled the high rate of reaction. The whiteline intensity of oxidized platinum in case of Pt-773 is less than in Pt-623, which suggests that 2.3 nm particles are not oxidized as deeply as 0.7 nm particles, which correlates to the surface oxidation of particles [42]. The intense features after the whiteline, at 11,585 and 11,595 eV, compared to Pt-623 also suggested that even in the high-activity region the spectra still had contributions from the relatively large platinum core. There is evidence of these results using full EXAFS analysis for particle size effects on the extent of oxidation in the high-activity region [42].

Our experiments show that regardless of the particle size, as studied here, in the low-activity region, below ignition temperatures, the surface is covered with CO and the reaction rate is low and determined by the desorption of CO. At these temperatures, the platinum particles are reduced with adsorbed CO, even in an O_2-rich environment. As the temperature increases, some of the CO desorbs from the platinum surface, which is reflected in the lower intensity of whiteline doublet in the HERFD spectra and in the blue shift of the stretching frequency of adsorbed CO in the IR data. At the ignition temperature, the rate increases suddenly and oxidic platinum forms. HERFD XAS is very sensitive to the particle size, as the doublet in the whiteline is pronounced only when the particle size is below or equal to 1 nm.

4. Conclusions

Platinum nanoparticles of different particle sizes, supported on alumina, and prepared by incipient-wetness impregnation, show different activities in the CO oxidation. In situ HERFD XAS and infra studies have distinguished the active phases in the low- and the high-activity regimes: platinum adsorbed with CO in the low-activity regime. In the low-activity region, the catalyst is poisoned by CO, thus limiting the reaction of CO. These results are consistent for different particle size. Also, the particle size effects the temperature of ignition, which in turn effects the activity of the catalyst towards CO oxidation. The higher conversion over the catalyst with the smaller particles is responsible for a lower coverage of CO enabling O_2 to react with the surface and start ignition at a lower temperature.

Acknowledgements

The authors thank Jeffrey T. Miller, Argonne National Laboratory, USA for providing the catalyst samples, Dr. Frank Krumeich, ETH Zurich, Switzerland for providing STEM micrographs of samples. The authors are also grateful to ESRF, France for beamtime at ID26, and to the Swiss National Science Foundation (SNF) for financial support.

References

[1] L.F. Mattheiss, R.E. Dietz, Phys. Rev. B 22 (1980) 1663.
[2] B. Delley, D.E. Ellis, A.J. Freeman, E.J. Baerends, D. Post, Phys. Rev. B 27 (1983) 2132.
[3] M.G. Mason, Phys. Rev. B 27 (1983) 748.
[4] M. Kuhn, J.A. Rodriguez, J. Hrbek, A. Bzowski, T.K. Sham, Surf. Sci. 341 (1995) L1011.
[5] G.C. Bond, D.T. Thompson, Catal. Rev. Sci. Eng. 41 (1999) 319.
[6] N. Lopez, J.K. Nørskov, J. Am. Chem. Soc. 124 (2002) 11262.
[7] C.D. Dudfield, R. Chen, P.L. Adock, Int. J. Hydrogen Energy 26 (2001) 763.
[8] R.J. Farrauto, R.M. Heck, Catal. Today 51 (1999) 351.
[9] H. Hopster, H. Ibach, G. Comsa, J. Catal. 46 (1977) 37.
[10] E.C. Akubuiro, X.E. Verykios, L. Lesnick, Appl. Catal. 14 (1985) 215.
[11] D.N. Belton, S.J. Schmieg, Surf. Sci. 202 (1988) 238.
[12] A. Szabó, M.A. Henderson, J.T. Yates, J. Chem. Phys. 96 (8) (1992) 6191.
[13] G.S. Zafiris, R.J. Gorte, Surf. Sci. 276 (1992) 86.
[14] I. Stará, V. Nehasil, V. Matolín, Surf. Sci. 331–333 (1995) 173.
[15] V. Nehasil, I. Stará, V. Matolín, Surf. Sci. 352–354 (1996) 305.
[16] U. Heiz, A. Sanchez, S. Abbet, W.D. Schneider, J. Am. Chem. Soc. 121 (1999) 3214.
[17] I. Meusel, J. Hoffmann, J. Hartmann, J. Libuda, H.J. Freund, J. Chem. Phys. B 105 (2001) 3567.
[18] A.K. Santra, D.W. Goodman, Electrochim. Acta 47 (2002) 3595.
[19] J.L. Gland, M.R. McClellan, F.R. McFeely, J. Chem. Phys. 79 (1983) 6349.
[20] A. Szabo, M.A. Henderson, J.T. Yates, J. Chem. Phys. 96 (1992) 6191.
[21] D.W. Goodman, C.H.F. Peden, G.B. Fisher, S.H. Oh, Catal. Lett. 22 (1993) 271.
[22] M. Bowker, Q. Guo, Y. Li, R.W. Joyner, Catal. Lett. 22 (1993) 275.
[23] J.Z. Xu, J.T. Yates, J. Chem. Phys. 99 (1993) 725.
[24] G.S. Zafiris, R.J. Gorte, J. Catal. 140 (1993) 418.
[25] T.H. Lindstrom, T.T. Tsotsis, Surf. Sci. 150 (1985) 487.
[26] J.A. Anderson, J. Chem. Soc., Faraday Trans. 88 (8) (1992) 1197.
[27] R. Burch, P.K. Loader, Appl. Catal. A 122 (1995) 169.
[28] F.J. Gracia, L. Bollmann, E.E. Wolf, J.T. Miller, A.J. Kropf, J. Catal. 220 (2003) 382.
[29] M.D. Ackermann, T.M. Pedersen, B.L.M. Hendriksen, O. Robach, S.C. Bobaru, I. Popa, C. Quiros, H. Kim, B. Hammer, S. Ferrer, J.W.M. Frenken, Phys. Rev. Lett. 95 (2005) 255505.
[30] R. Burch, P.K. Loader, Appl. Catal. B 5 (1994) 149.
[31] S. Yang, A.M. Valiente, M.B. Gonzalez, I.R. Ramos, A.G. Ruiz, Appl. Catal. B 28 (2000) 223.
[32] C. Stampfl, M. Scheffler, Phys. Rev. Lett. 78 (1997) 1500.
[33] X.-G. Wang, A. Chaka, M. Scheffler, Phys. Rev. Lett. 84 (2000) 3650.
[34] K. Reuter, M. Scheffler, Phys. Rev. B 65 (2002) 035406.
[35] K. Reuter, M. Scheffler, Phys. Rev. B 68 (2003) 045407.
[36] H. Over, Y.D. Kim, A.P. Seitsonen, S. Wendt, E. Lundgren, M. Schmid, P. Varga, A. Morgante, G. Ertl, Science 287 (2000) 1474.
[37] X. Su, P.S. Cremer, Y.R. Shen, G.A. Somorjai, J. Am. Chem. Soc. 119 (1997) 3994.
[38] P.-A. Carlsson, L. Oesterlund, P. Thormaehlen, A. Palmqvist, E. Fridell, J. Jansson, M. Skoglundh, J. Catal. 226 (2004) 422.
[39] F.J. Gracia, S. Guerrero, E.E. Wolf, J.T. Miller, A.J. Kropf, J. Catal. 233 (2005) 372.
[40] P.-A. Carlsson, V.P. Zhdanov, M. Skoglundh, Phys. Chem. Chem. Phys. 8 (2006) 2703.
[41] J. Singh, E.M. Alayon, M. Tromp, O. Safonova, P. Glatzel, M. Nachtegaal, R. Frahm, J.A. van Bokhoven, Angew. Chem. Int. Ed. 47 (2008) 9260.
[42] E.M. Alayon, J. Singh, M. Nachtegaal, M. Harfouche, J.A. van Bokhoven, J. Catal. 263 (2009) 228.
[43] D.M. Haaland, F.L. Williams, J. Catal. 76 (1982) 450.
[44] P.T. Fanson, W.N. Delgass, J. Lauterbach, J. Catal. 204 (2001) 35.
[45] Y. Barshad, X. Zhou, E. Gulari, J. Catal. 94 (1985) 128.
[46] N.W. Cant, D.E. Angove, J. Catal. 97 (1986) 36.
[47] Y.-E. Li, D. Boecker, R.D. Gonzalez, J. Catal. 110 (1988) 319.
[48] J. Sarkany, R.D. Gonzalez, Appl. Catal. 5 (1983) 85.
[49] J. Sarkany, M. Bartok, R.D. Gonzalez, J. Catal. 81 (1983) 347.

[50] J.A. Anderson, Catal. Lett. 13 (1992) 363.
[51] D.E. Ramaker, D.C. Koningsberger, Phys. Rev. Lett. 89 (2002) 139701.
[52] A.L. Ankudinov, J.J. Rehr, J.J. Low, A.R. Bare, Phys. Rev. Lett. 89 (2002) 139702.
[53] M.K. Oudenhuijzen, J.A. van Bokhoven, J.T. Miller, D.E. Ramaker, D.C. Koningsberger, J. Am. Chem. Soc. 127 (2005) 1530.
[54] O.V. Safonova, M. Tromp, J.A. van Bokhoven, F.M.F. de Groot, J. Evans, P. Glatzel, J. Phys. Chem. B 110 (2006) 16162.
[55] P. Glatzel, U. Bergmann, Coord. Chem. Rev. 249 (2005) 65.
[56] F.M.F. de Groot, Coord. Chem. Rev. 249 (2005) 31.
[57] J.A. van Bokhoven, C. Louis, J.T. Miller, M. Tromp, O.V. Safonova, P. Glatzel, Angew. Chem. Int. Ed. 45 (2006) 4651.
[58] J. Singh, M. Tromp, O. Safonova, P. Glatzel, J.A. van Bokhoven, Catal. Today 145 (2009) 300.
[59] N. Weiher, E. Bus, B. Gorzolnik, M. Möller, R. Prins, J.A. van Bokhoven, J. Synchr. Rad. 12 (2005) 675.
[60] N. Sheppard, T.T. Nguyen, in: R.J.H. Clark, R.E. Hester (Eds.), The Vibrational Spectra of CO Chemisorbed on the Surfaces of Metal Catalysts—A Suggested Scheme of Interpretation, vol. 5, Heyden, London, 1978, p. 67.
[61] A. Crossley, D.A. King, Surf. Sci. 68 (1977) 528.
[62] P. Hollins, J. Pritchard, Prog. Surf. Sci. 19 (4) (1985) 275.
[63] P. Araya, W. Porod, E.E. Wolf, Surf. Sci. 230 (1990) 245.
[64] M.S. Chen, Y. Chai, Z. yan, K.K. Gath, S. Axnanda, D.W. Goodman, Surf. Sci. 601 (2007) 5326.
[65] L.-C. deMénorval, A. Chaqroune, B. Coq, F. Figueras, J. Chem. Soc., Faraday Trans. 93 (1997) 3715.
[66] G. Blyholder, J. Phys. Chem. 68 (1964) 2773.
[67] R.K. Brandt, M.R. Hughes, L.P. Bourget, K. Truszkowska, R.G. Greenler, Surf. Sci. 286 (1993) 15.
[68] M.J. Kappers, J.H. van der Maas, Catal. Lett. 10 (1991) 365.
[69] T. Lear, R. Marshall, J.A.L. Sanchez, S.D. Jackson, T.M. Klapötke, M. Bäumer, G. Rupprechter, H.-J. Freund, D. Lennona, J. Chem. Phys. 123 (2005) 174706.